



Salman, M. A. T. S., & Pearson, M. (2017). Advancing whisker based navigation through the implementation of Bio-Inspired whisking strategies. In *2016 IEEE International Conference on Robotics and Biomimetics (ROBIO 2016): Proceedings of a meeting held 3-7 December 2016, Qingdao, China* Institute of Electrical and Electronics Engineers (IEEE). <https://doi.org/10.1109/ROBIO.2016.7866416>

Peer reviewed version

Link to published version (if available):
[10.1109/ROBIO.2016.7866416](https://doi.org/10.1109/ROBIO.2016.7866416)

[Link to publication record in Explore Bristol Research](#)
PDF-document

This is the author accepted manuscript (AAM). The final published version (version of record) is available online via IEEE at <http://ieeexplore.ieee.org/document/7866416/>. Please refer to any applicable terms of use of the publisher.

University of Bristol - Explore Bristol Research

General rights

This document is made available in accordance with publisher policies. Please cite only the published version using the reference above. Full terms of use are available:
<http://www.bristol.ac.uk/red/research-policy/pure/user-guides/ebr-terms/>

Advancing whisker based navigation through the implementation of Bio-Inspired whisking strategies

Mohammed Salman¹ and Martin J. Pearson¹

Abstract—An active whisking tactile sensor array has been successfully integrated with the RatSLAM algorithm and demonstrated as capable of reducing error in pose estimates of a mobile robot. A new metric for evaluating the performance of RatSLAM is introduced in order to evaluate the impact in performance of whisker-RatSLAM through the adoption of a biomimetic active whisker control scheme and different approaches to tactile sensory pre-processing. Improvements in performance are presented and discussed with respect to how whisker-RatSLAM could form the basis of a computationally efficient and robust localisation and mapping algorithm to adopt for tactile robotic exploration.

I. INTRODUCTION

The environment within burning or recently collapsed buildings contains dense and irregular concentrations of suspended particulates that limit the perceptual ability of visual and laser based sensory systems. Further, the confined and unstructured nature of such scenarios also confounds active acoustic and near field radar sensing. Animals tend to rely heavily on their sense of touch when navigating through such environments [1] which serves as an intriguing existence proof for the development of artificial tactile sensory solutions. We advocate the use of a whisker based sense of touch due to the inherent fault tolerance and extended reach compared to sub-cutaneous based tactile sensors modeled on the human finger-tip. Previous work has demonstrated that small scale regions of previously unexplored space can be mapped and simultaneous improvements made to pose estimates using whisker based sensors on mobile robots [2], [3], however, large scale tactile mapping still presents significant challenges due to scene ambiguity and memory requirement for dense metric map representations. Here we evaluate RatSLAM [4] as the computational basis for deriving best estimate of map and pose using an array of active whiskers mounted as the end effector to a 6DoF manipulator. RatSLAM was chosen due to its low computational cost and potential for multi-modal sensory extension. Designed originally to receive visual sensory input and based on known principles of neural dynamics and anatomy, it has been demonstrated robustly mapping large areas of urban landscape [4]. Our ultimate ambition is to carry out 6D SLAM with the whisker array being the primary sensor for environmental perception. In this paper we describe how an active tactile whisker array and robotic arm have been successfully integrated with the RatSLAM algorithm and how the performance of this system at building a map and

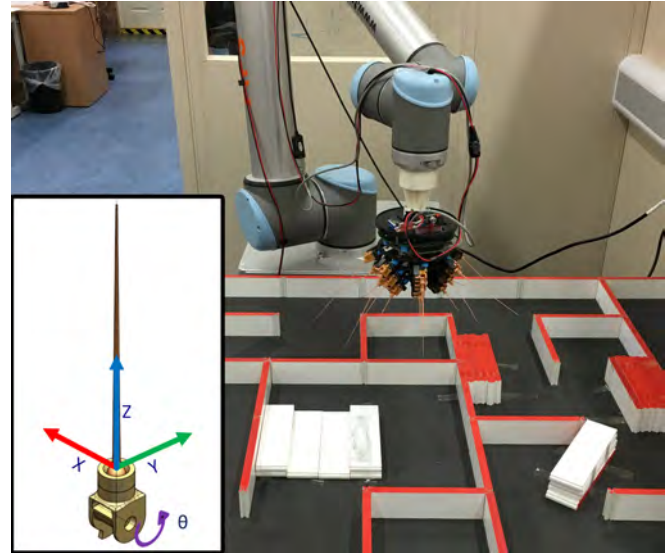


Fig. 1: Whiskered head mounted on UR-10 arm and positioned above a maze used to evaluate the whisker-RatSLAM algorithm. **Inset)** Individual whisker highlighting reference frame for whisker deflection (x , y) and whisker rotation (θ)

maintaining an estimate of location can be quantified. The robustness of the whisker-RatSLAM system was also tested to evaluate its performance when faced with challenging behavioral paradigms such as reverse tracking and kidnapped robot. Finally, a metric is developed to quantify and compare the system performance following the adoption of an active whisker control strategy derived from direct ethological observation of rat whiskers. In summary the aim of this paper is to show that whisker data may be integrated with RatSLAM and that given the adoption of bio-inspired whisker strategies the system is able to improve its SLAM performance.

II. BACKGROUND

A. RatSLAM

Given that a mobile agent is tasked with navigating an unknown environment, there needs to be a process that enables it to construct a map and locate itself within it. Such a process is popularly known as Simultaneous Localization and Mapping (SLAM) [5]. The process involves the fusion of noisy sensory data from multiple sources in order to produce a more precise estimate of the map and the agents pose. Most commonly adopted SLAM algorithms are based on derivatives of the Bayes filter whereby the belief of a given map and pose are recursively updated in response to robot motion and

¹Bristol Robotics Laboratory, University of Bristol and University of the West of England, Bristol, UK

sensory observation (such as in Kalman and Particle filters). In contrast to these purely probabilistic methods, RatSLAM is based on a simplified rodent hippocampus model that uses the principles of place, grid and head direction cells in conjunction with visual and self motion feedback to perform SLAM. By associating visual cues with the pose at the time of obtaining said cues, a connection can be made when the same visual cue is experienced. Thereby, a correction to the current pose estimate is made possible by recalling the pose of the previously associated visual cue. To derive this best estimate of robot pose based on motor command, visual cues and prior experience, RatSLAM uses a substrate inspired by a continuous attractor model of neural dynamics [4]. This is based on the well known center surround pattern of neural connectivity reported in many regions of the brain [6] which introduces an intriguing opportunity for future exploration into how this algorithm is physically implemented, particularly with regards to the adoption of low powered neuromorphic computing platforms [7].

B. Whiskers

Many small mammals use their prominent array of facial whiskers to explore their environment through the sense of touch. They actively move their whiskers with a rhythmic back and forth motion (known as *whisking*) in order to extend their sensory range and to palpate the surface of objects that they encounter [8]. The regular rhythmic pattern of whisking observed as these animals explore free space is actively perturbed when contacts are made with unexpected objects [9]. Specifically, a whisker that makes contact will express Rapid Cessation of Protraction (RCP), in other words, the whisker will be prevented from moving further forwards into the point of contact. In addition, the whiskers that have not made contact, for example the whiskers on the side of the array that are contra-lateral to the contacting whisker, will be protracted further toward the point of contact. Together these close coupled sensorimotor responses implement a behavioral strategy known as *minimal impingement, maximal contact* [9], which, it has been proposed, attempts to maximise the quantity and quality of information available from an array of whisker sensors [10]. The quantity of information from a whisker array is increased by maximizing the frequency of whisker contacts with objects in the environment and can be clearly observed and measured. The quality of the sensory information however is less clearly defined and is highly dependent on the context of the current task that is being performed. It has been suggested that RCP may improve the quality of sensory information by normalizing the magnitude of deflection of the whisker shaft following contact thereby constraining the range of sensory response to a region best suited for signal processing, however, so far this has not been empirically demonstrated. More pragmatically, the introduction of an RCP-like mechanism for artificial active whiskers is desirable as it leads to a significant improvement in physical robustness of the array due to reduced whisker damage. Research has also shown that the frequency of

vibration of whiskers may be used in the identification of textural features [11], which makes low noise deflection data desirable. Therefore, by implementing a control loop that reproduces RCP in an artificial whisker array and deploying that model in a real world task, such as mapping in this case to increase robustness of the system, we also have the opportunity to quantify task performance that may be informative to biology.

III. METHOD

Initial runs were made to determine the outcome of fusing the whisker's contact images with RatSLAM. A RatSLAM specific performance metric based on experience history, henceforth referred to as Experience Metric (ExM), is validated and used to evaluate the following experiments. Experiments were then conducted to gather data sets to evaluate any improvement in the RatSLAM algorithm performance through the application of the biologically inspired whisker movement strategies and the method in which whisker images are generated.

A. The platform

The Platform consists of a 6DoF robotic manipulator (Universal Robotics UR-10) and a whiskered *head module* that was mounted as its end effector as shown in Figure 1. The head module, measuring $130 \times 164 \times 210$ mm, consists of 18 whiskers arranged into 3 concentric circles of 6 (measuring 50 mm, 110 mm, 160 mm in length within each circle) that are individually driven via DC motors. Each whisker returns three sensor readings that include the whisker rotation angle θ , and the deflection force felt at its shaft in the x and y direction, as indicated in the inset panel of Figure 1. The robotic manipulator returns regular reports of the absolute position of the end effector which were used to calculate the average velocity of the end effector between each given interval.

B. System Integration

The subsystems were integrating using the framework provided by the Robot Operating System (ROS). The RatSLAM algorithm was adapted to work with ROS by the authors of OpenRatSLAM [12] and initiated the appropriate listener for streaming in the odometry and 'visual' data.

The head module was connected, via USB, to a custom built PC to minimise data transfer latency. However, this subsystem was not compatible with ROS, therefore the sensory data needed to be transferred in the form of CSV files via the local network to a second computer that would create the whisker image topic that OpenRatSLAM is programmed to listen to. A similar method of editing data files across the local network could be used for dynamically changing the whisking parameters although for the following experiments this was not needed.

The UR-10 arm is compatible with ROS and the manipulator specific plug-in, *MoveIt*. This plug-in provides the necessary functions for trajectory planning and calculating end effector position, the derivative of the latter used to compute the linear

and angular velocity of the head module required to drive the OpenRatSLAM algorithm. The raw odometry data is also streamed to its dedicated topic and was used to reconstruct the ground truth of robot trajectory.

C. Experimental Setup

The whiskered robot was positioned above a $1.35 \times 1m$ re-configurable maze composed of plastic walls and posts that conform to the rules of the micromouse competition [13]. The height of the whiskered head module was fixed 7.7 cm above the maze such that the whiskers would only make contact with the walls during active whisking and not the maze floor. The head module was then translated around a maze, according to a predetermined path (shown in Figure 2) whilst the whiskers were actively whisked at approximately 1 Hz (i.e., 1 whisk cycle per second). Following a number of preliminary runs to tune the parameters of the RatSLAM algorithm, a series of data sets were gathered as the head module was moved along the predetermined path in 3 clockwise circuits, followed by 3 anti-clockwise circuits, and then 2 alternating clockwise, anti-clockwise circuits. Therefore, a group of ten such circuits constituted a complete data set; of which three were gathered with the whisking control in open loop and three whilst the whisking was modulated using a biomimetic model of RCP (described below). The whisker angle (θ) and deflection vector (x, y) from each of the 18 whiskers on the head module were sampled at 2 kHz throughout each 10 circuit run along with the odometry from the UR-10 arm sampled at 1 Hz. The whisker data was processed using 2 different approaches (described below) in order to generate a “visual” representation of the tactile scene required by OpenRatSLAM. The odometry from the UR-10 was converted into 2 average velocities (translation and rotation) again required as input to the RatSLAM algorithm. The effect of integrating the low sampled odometry resulted in a perceived pose that was erroneous. The characterization of this noise was calculated to have a normal distribution for the error in linear displacement $\mathcal{N}(0, 8.2)$ in mm and a normal distribution for the angular displacement $\mathcal{N}(0, 1.03e^{-1})$ in radians. The impact of this error is highlighted in the deviation of path estimate from the ground truth shown in Figure 2.

D. Whisker tactile to image transform

The problem of tactile representation is non trivial and has been studied by others [14]. For our purposes we opted to represent the tactile information as single point contacts occurring at the tip of each whisker. The whisker sensory data was transformed into equivalent visual images for the RatSLAM algorithm by representing each whisker as a pixel in a 3×6 pixel image. The intensity of each pixel was proportional to the approximate vertical height of any obstacle detected using a measure of whisker angle, θ , at point of contact and the forward kinematics of the specific whisker. The angle of contact was derived at the end of each whisk cycle using 2 approaches; the first, which we called *max_angle*, was taken as the maximum

whisker angle reported during the cycle; the second, known as *contact_angle* measured when the magnitude of the first derivative of the whisker deflection crossed a threshold as the time of contact incidence. The angle of the whisker at that time in the whisk cycle was then passed through the forward kinematics to determine depth. We found that *max_angle*, was robust to sensor noise, however, it did reduce the frequency of positive wall detection as the whisker must remain in contact with the wall for the duration of the whisk cycle. By contrast *contact_angle* generated a larger number of contact measurements, however, was susceptible to sensor noise and therefore spurious observations.

E. Whisker motion control

The two modes of whisker control that were used between the different data sets were called *open-loop* and *RCP*. Open-loop mode consisted of simple trajectory tracking of each whisker angle following a sinusoidal 1 Hz pattern of fixed magnitude. RCP mode received the same desired trajectory, however, the actual whisk angle of each whisker could also be perturbed by local feedback from the whisker deflection sensors themselves. The magnitude of the perturbation was defined as the absolute average deflection, in the y direction, that exceeded the contact threshold. The contact threshold was calculated at time of calibration as \pm twenty times the standard deviation of the recorded noise from the mean of the deflection data during *free-whisking*, i.e., whilst the whiskers were whisking at 1 Hz in absence of any obstacles. An increase in perturbation resulted in a decrease of whisking amplitude, while keeping the initial whisking angle at the start of each cycle constant. Keeping the initial whisk angle constant is desirable as it meant the whiskers average angle was kept slightly higher than the tallest obstacle and thus reduced the chances of any whiskers getting trapped within the maze’s walls.

F. OpenRatSLAM Parameters

Before assessing the performance of the algorithm with a given data set, the OpenRatSLAM parameters need to be tuned in order to achieve the best performance possible. This tuning process mainly deals with two parameters, which are the visual template matching threshold and the pose cell inject energy. The *visual template matching threshold* parameter refers to the threshold used to define whether two separate visual templates are similar. Due to the coarseness of the whisker image (compared to visual images) a low value must be selected in order to prevent false matches. When a visual template is matched, the activity in the associated pose cell is increased (see [4] for detail). The *pose cell inject energy parameter*, therefore, affects how much this activity is increased, which in turn controls frequency of re-localisation of the algorithm. RatSLAM tuning was achieved by reducing the pose cell injection energy parameter to a low value (half of what’s implemented in the *iRat* data set [12]) and steadily increasing the visual template matching threshold until RatSLAM is able to close the first loop without any *incorrect* re-localizations.

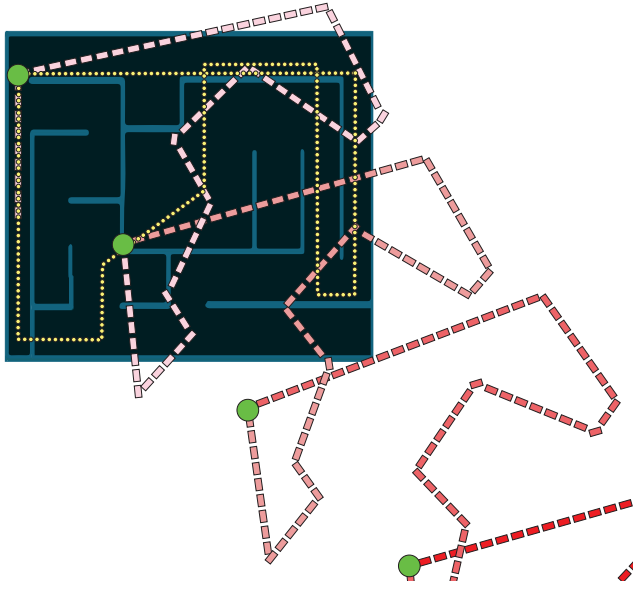


Fig. 2: Actual path taken by the whisker module (circular dashes) and the path derived from integrated odometry data (rectangular dashes), the latter of which was cropped to only include the first three clockwise loops. Each loop increases in color saturation in order to show their progression in time additionally a large circle marks the start/end of a loop. The image highlights the effects that accumulating small odometry error has on the estimation of robot pose and thus a need for an adequate SLAM technique.

G. Performance Metrics

Two metrics were used to quantitatively assess the performance of the RatSLAM algorithm. The first metric, which we called the *Experience Metric* (ExM), is novel and was designed specifically for use with the RatSLAM algorithm while the second, *Energy Metric* (EM), was derived from [15] as is a more general metric for evaluating SLAM algorithms. The reasons for introducing the Experience Metric is revealed in the results and described further in the discussion section of this paper, here we simply describe the principles of the new metric and the existing Energy Metric.

A bench mark visual data set was taken from an online repository [16] (and described here [17]), to serve as a sanity check for discussion of the more general performance of whisker based SLAM. The *iRat* data set was selected because it was derived from a similarly sized environment to the maze used here, as well as containing ground truth pose data.

1) *Experience Metric (ExM)*: Figure 3 shows the dynamics of experiences throughout the entire run of the *iRat* data set, with each experience given a unique ID number. A dip in experience is defined as a re-localization as the agent perceives a return to a previous pose. In order to assess the correctness of the re-localization, a series of experiences that define the main loop closure must be selected. This is needed as future re-localizations return to these base set of experiences (The experience IDs preceding the vertical line in Figure 3). A re-localization is thus defined as being correct

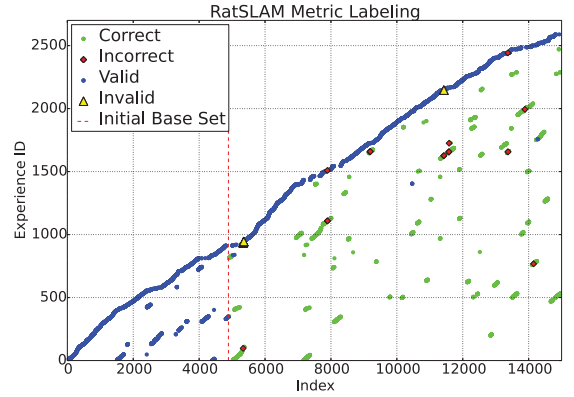


Fig. 3: RatSLAM Metric Labeling. The image shows how RatSLAM associates the agents current position and observations with an experience ID. An experience ID that is visited more than once signifies a re-localization and is considered *correct* or *incorrect* based on the specifications of the user regarding their desired accuracy in pose. Novel experiences following an *incorrect* re-localization are deemed *invalid* as their accuracy can't be validated until a *correct* re-localization occurs.

provided the difference between its perceived and actual position and angle are below a threshold. In order to take into account for future trajectories through areas that have not yet been visited, the new experiences are placed within a set of *valid* experiences provided that they are preceded by a *correct* re-localization. If an *incorrect* re-localization occurs, experiences following it are considered *invalid* and future re-localizations to this set are also considered *incorrect*.

ExM returns two values, the Average Rate of Re-localization (ARR) and the Average Rate of Correct Re-localization (ARCR). ARR is defined as the average number of re-localizations over the total number of experiences not including the original base set. ARCR is defined as the average number of correct re-localizations over the total number of re-localizations. A number close to one for both these metrics indicates that the agent has high confidence in its pose estimate. For the proceeding results, the thresholds for position and angular accuracy were $0.1m$ and 25° respectively. The outputs are derived using Algorithm 1.

2) *Energy Metric (EM)*: The Energy metric was derived from [15]. The authors measured the performance of a SLAM algorithm by defining the energy that it takes to transform the trajectory of the agent according to the SLAM algorithm to, ideally, the true trajectory of the agent. The Energy Metric is defined by Equation 1 where N is the number of relative relations (an experience point in the RatSLAM experience map and its corresponding sample point from the set of collected pose data). The variable $\delta_{i,j}$ is defined in Equation 2 and is the relative transformation from node x_i to node x_j . The functions $trans(\cdot)$ and $rot(\cdot)$ refer to translation and rotation respectively. The Energy Metric indicates a good performance by returning a low value, with zero being a run that resulted in no error at all.

Algorithm 1: Experience Metric

```

1 function ExperienceMetric ( $\mathbf{E}, \mathbf{P}, i_{base}, \delta_p, \delta_\theta$ )
  Input : Experience Log  $\mathbf{E} = (e_1 e_2 \dots e_n)$ 
           Ground Truth Log  $\mathbf{P} = (\mathbf{p}_\theta, \mathbf{p}_x, \mathbf{p}_y)$ 
            $i_{base}$  = final index of base set in  $\mathbf{E}$ 
            $\delta_p$  = position error threshold
            $\delta_\theta$  = angular error threshold
  Output: Average rate of correct relocalization  $\psi_c$ 
           Average rate of relocalization  $\psi_r$ 

2  $\mathbf{C} = \text{unique}(\mathbf{E}[1 : i_{base}])$  // Remove duplicates
3  $\eta_c, \eta = 0$ 
4  $r_c = \text{True}$ 
5 for  $i = i_{base} + 1$  to  $n$  do
6    $e_{i-1} = \mathbf{E}[i - 1]$ 
7    $e_i = \mathbf{E}[i]$ 
8    $\mathbf{E}_{past} = (e_1 \dots e_{i-1})$ 
9    $\kappa_{r1} = e_i \in \mathbf{E}_{past}$ 
10   $\kappa_{r2} = (e_i = e_{i-1}) \wedge (e_{i-1} \notin \mathbf{R})$ 
11  if  $\kappa_{r1}$  and not  $\kappa_{r2}$  then
12     $\mathbf{R}[\eta] = e_i$  // Relocalization
13     $\eta++$ 
14  end
15  if  $e_i \in \mathbf{R}$  then
16     $p_{true} = (\mathbf{p}_x[i], \mathbf{p}_y[i])$  // Ground Truth
17     $\theta_{true} = (\mathbf{p}_\theta[i])$ 
18     $i_{past} = \text{for } e \text{ in } \mathbf{E}_{past} [j = 1 \dots i - 1] \text{ return last } j \text{ where } e = e_i$  // Perceived
19     $p_{perceived} = (\mathbf{p}_x[i_{past}], \mathbf{p}_y[i_{past}])$ 
20     $\theta_{perceived} = (\mathbf{p}_\theta[i_{past}])$ 
21     $\epsilon_p = \text{norm}(p_{true} - p_{perceived})$  // Euclidean
22     $\epsilon_\theta = \text{abs}(\theta_{true} - \theta_{perceived})$  // Absolute
23     $\kappa_{c1} = (e_i \in \mathbf{C}) \wedge ((\epsilon_p < \delta_p) \wedge (\epsilon_\theta < \delta_\theta))$ 
24     $\kappa_{c2} = (e_i = e_{i-1}) \wedge (e_{i-1} \in \mathbf{R}_c)$ 
25    if  $\kappa_{c1}$  and  $\kappa_{c2}$  then
26       $\mathbf{R}_c[\eta_c] = e_i$  // Correct relocalization
27       $\eta_c++$ 
28       $r_c = \text{True}$ 
29    else
30       $r_c = \text{False}$ 
31    end
32  end
33  if  $r_c$  then
34    if  $e_{i-1} \notin \mathbf{C}$  then
35       $\text{append } \mathbf{C} \text{ with } e_{i-1}$ 
36    end
37  end
38 end
39  $\eta_{exp} = \text{length}(\mathbf{E}) - i_{base}$ 
40  $\psi_r = \eta / \eta_{exp}$  // ARR
41  $\psi_c = \eta_c / \eta$  // ARCR

```

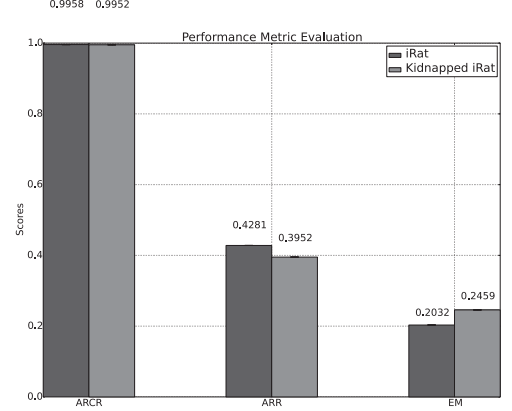


Fig. 4: Performance Metric Validation. The results show that for a manipulated data set designed to reduce the performance of the RatSLAM algorithm, ExM does indeed show a reduction in performance via a reduction in the frequency of re-localizations (ARR). This reduction of performance is also observed by the increase in Energy Metric [15].

$$\varepsilon(\delta) = \frac{1}{N} \sum_{i,j} \text{trans}(\delta_{i,j} \ominus \delta_{i,j}^*)^2 + \text{rot}(\delta_{i,j} \ominus \delta_{i,j}^*)^2 \quad (1)$$

$$\delta_{i,j} = x_j \ominus x_i \quad (2)$$

IV. RESULTS

A. Performance Metric Evaluation

ExM was evaluated using the *iRat* data set. The data set was replicated and modified by “kidnapping” the agent, i.e., skipping it forward to a future position, thereby creating two data sets for comparison, the latter set should result in a reduction of performance to confirm the correctness of the metric. EM was also used to measure the reduction in performance of the algorithm for comparison. The results of this test is shown in Figure 4, which by the decrease in ARR from the ExM and increase in EM, indicates the expected drop in performance. The decrease in ARR may be attributed to the fact that the chain of “visual” scenes that leads to a re-localization was disrupted by the kidnapping and thus temporarily prevented any re-localization. In the case of EM, RatSLAM was penalized for not detecting the kidnapping immediately, which led to the increase in error. ARCR remained relatively constant, which indicated that the RatSLAM parameters were appropriately tuned to correctly associate “visual” templates. With confirmation of a valid metric behavior, it was then be used for a quantitative evaluation of the impact on performance of whisker-RatSLAM through the adoption of the different whisker tactile to image transforms and whisker motion control schemes.

B. Vanilla Whisker-RatSLAM Performance

Using the simple open-loop mode of whisker control and the max_angle scheme for whisker tactile to image transform, Whisker-RatSLAM was proven capable of accommodating

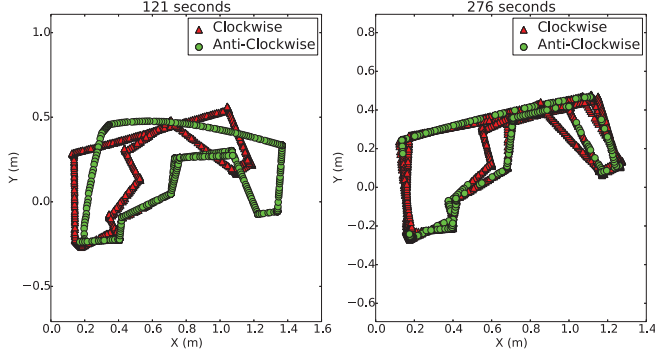


Fig. 5: Plots showing trajectory estimates derived from whisker-RatSLAM following multiple runs of alternate robot loop directions (clockwise in red and anticlockwise in green). The **Left** plot emphasizes how the different directions of travel generate significantly different estimates of path trajectory. However, this difference reduces in **Right** panel following repeated iterations of loop closure in both directions. This was due to links being made between points of similarity in the maze leading to re-localization through shared experiences, which was particularly apparent at the turning points in the trajectory

the relatively sparse sensory information from the whisker “tactile images” by demonstrating loop closure and expressing only a limited number of *incorrect* re-localizations, as indicated by the transition from the erroneous path in Figure 2 to the corrected path in Figure 5. An impressive feat given the ambiguity in the features present in the maze environment. When faced with changes to path direction, it was observed that for all data sets, experiences created when driven in an anti-clockwise direction were not associated with their clockwise counterparts, instead they were treated as unique locations. By alternating the path direction multiple times, the separate loops from the clockwise and anticlockwise runs began to overlap as the agent observed similar tactile images when rotating at corners. This scenario of overlap can be seen in Figure 5.

C. Whisker Control

The following set of results compare the performance of the robot when its whiskers are controlled using the *open-loop* and *RCP* schemes described earlier.

Figure 6 shows that the adoption of *RCP* whisker control improves the performance of the whiskered robot by making frequent *correct* re-localizations as indicated by the increase in *ARR* values from 0.1765 to 0.2257. *ARCR* on the other hand remained constant regardless of the whisker control scheme. The improvement in performance through the adoption of *RCP* based whisker control was also measured using *EM* as a decreased average measure of 0.1916 to 0.1568 across all data sets.

D. Whisker Contact Angle

The previous runs were processed such that the whisker image was constructed based on the *max_angle* method,

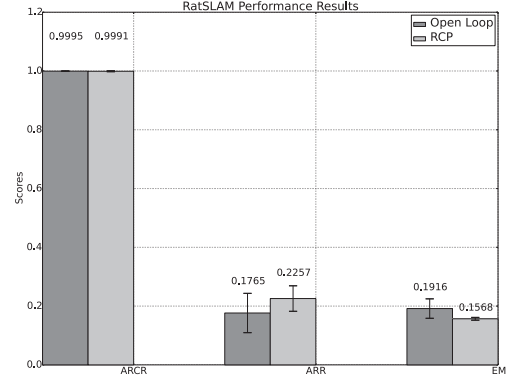


Fig. 6: RatSLAM Performance comparison between Open Loop and *RCP* whisker control. Increasing *ARCR* and *ARR* and decreasing *EM* indicate improvement in performance.

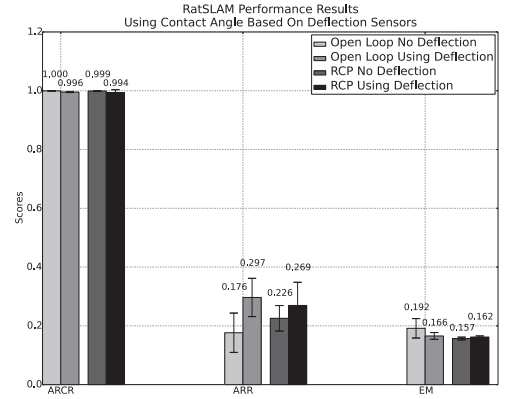


Fig. 7: RatSLAM Performance Results Using *contact_angle* - Increasing *ARCR* and *ARR* and decreasing *EM* indicate improvement in performance.

the following results are however the results of the second method *contact_angle*.

ExM shows a clear improvement in performance with increasing *ARR* values for both *open-loop* and *RCP* variations as shown in Figure 7. *Open-loop* *ARR* value is also observed to be greatly increased following the use of *contact_angle*. *EM* performance shows slight improvement in the case of *open-loop*, unlike *RCP*, which shows a very small reduction in performance. The visual template matching threshold was increased during the use of *contact_angle*, which suggested a reduction in ‘image’ ambiguity.

V. DISCUSSION

This paper reports three novel contributions; first, the fusion of active whisker tactile data with the vision based RatSLAM by transforming contact height detected by the whiskers into pixel intensity; secondly, the introduction of a RatSLAM specific performance evaluation algorithm, the validity of which has been confirmed using the Energy

Metric from [15]; and third, an empirical evaluation of a biomimetic whisker control strategy.

The ultimate ambition of this research is to develop a system that is capable of building a map of its environment and maintaining an accurate estimate of its location through whisker based touch using minimal computational resources. Through the adoption of the RatSLAM algorithm we have demonstrated that this light weight algorithm has the potential for further investigation as a substrate for efficient tactile mapping and localisation. Further, we can now empirically evaluate the change in performance of RatSLAM in response to different sensory placement strategies and pre-processing schemes by measuring the dynamics of experience association within the algorithm. Theoretically, if RatSLAM were to map the environment completely it would create no further experiences, instead associating each new visual/tactile image with a previous experience and therefore re-localising confidently. This condition would be indicated by the ExM metric returning a ARR value of 1 and would be visualised in Figure 3 as an absence of new experiences following the establishment of the initial base set (as indicated by the red dotted line). In addition if the algorithm were performing perfectly all re-localisations would be deemed correct and therefore the ExM ARCR would also be 1. This ability to decompose the performance of the RatSLAM algorithm highlights the advantage of using the Experience Metric over the more generic Energy Metric.

Future work includes the investigation of RatSLAM's performance given perturbations in path trajectory for multiple loops. In the case of visual data sets, slight variations in pose at a given location was dealt with by calculating the visual template threshold for a set of translated images. Application of such a strategy in regards to the whisker image needs to be investigated in hopes of improving system robustness for the purpose of tackling the problems associated with navigating complex three dimensional environments. One method includes the extraction of contact features such as surface texture which maybe derived through analysis of the frequency of whisker vibration following contact. A complex undulating terrain is to be constructed in order to conduct these investigations as well as provide an alternative scenario that can corroborate the results of this paper. Additional whisker control strategies that have yet to be implemented include Spread Reduction [18], which should allow for the increase of whisking rate and thus sampling rate of the odometry. A higher sampling rate would result in additional contacts being made and more precise odometry measurements, thus theoretically improving the performance of the system. The aim of these investigations is to achieve a performance level that satisfies the requirements for carrying out 6D SLAM with the whisker array as the primary sensor for environmental perception.

ACKNOWLEDGMENT

This work was jointly supported by the EPSRC funded Centre for Doctoral Training in Robotics and Autonomous

Systems (Farscope) and the EU flagship the "Human Brain Project"

REFERENCES

- [1] J. H. Solomon and M. J. Hartmann, "Biomechanics: Robotic whiskers used to sense features," *Nature*, vol. 443, no. 7111, pp. 525–525, 10 2006. [Online]. Available: <http://dx.doi.org/10.1038/443525a>
- [2] C. Fox, M. Evans, M. Pearson, and T. Prescott, "Tactile SLAM with a biomimetic whiskered robot," in *IEEE Int. Conf. Robotics and Automation (ICRA)*, May 2012, pp. 4925–4930.
- [3] M. J. Pearson, C. Fox, J. C. Sullivan, T. J. Prescott, T. Pipe, and B. Mitchinson, "Simultaneous localisation and mapping on a multi-degree of freedom biomimetic whiskered robot," in *Robotics and Automation (ICRA), 2013 IEEE International Conference on*. IEEE, 2013, pp. 586–592.
- [4] M. Milford and G. Wyeth, "Mapping a suburb with a single camera using a biologically inspired slam system," *Robotics, IEEE Transactions on*, vol. 24, no. 5, pp. 1038–1053, Oct 2008.
- [5] H. Durrant-Whyte and T. Bailey, "Simultaneous localization and mapping: part i," *Robotics Automation Magazine, IEEE*, vol. 13, no. 2, pp. 99–110, June 2006.
- [6] D. H. Hubel and T. N. Wiesel, "Receptive fields, binocular interaction and functional architecture in the cat's visual cortex," *The Journal of Physiology*, vol. 160, no. 1, pp. 106–154, 1962. [Online]. Available: <http://dx.doi.org/10.1113/jphysiol.1962.sp006837>
- [7] E. Painkras, L. A. Plana, J. Garside, S. Temple, S. Davidson, J. Pepper, D. Clark, C. Patterson, and S. Furber, "Spinnaker: A multi-core system-on-chip for massively-parallel neural net simulation," in *Custom Integrated Circuits Conference (CICC), 2012 IEEE*, Sept 2012, pp. 1–4.
- [8] R. W. Berg and D. Kleinfeld, "Rhythmic whisking by rat: Retraction as well as protraction of the vibrissae is under active muscular control," *J Neurophysiol*, vol. 89, no. 1, pp. 104–117, Jan 2003.
- [9] B. Mitchinson, C. Martin, R. Grant, and T. Prescott, "Feedback control in active sensing: rat exploratory whisking is modulated by environmental contact," *Proceedings of the Royal Society, B*, vol. 274, pp. 1035–1041, 2007.
- [10] M. Pearson, B. Mitchinson, A. Pipe, and T. Prescott, "Biomimetic vibrissal sensing for robots," *Phil. Trans. of the Royal Society, B*, vol. 366, pp. 3085–3096, 2011.
- [11] N. Lepora, M. Pearson, B. Mitchinson, M. Evans, C. Fox, A. Pipe, K. Gurney, and T. Prescott, "Naive bayes novelty detection for a moving robot with whiskers," in *Robotics and Biomimetics (ROBIO), 2010 IEEE International Conference on*, Dec 2010, pp. 131–136.
- [12] D. Ball, S. Heath, J. Wiles, G. Wyeth, P. Corke, and M. Milford, "OpenratSLAM: an open source brain-based slam system," *Autonomous Robots*, vol. 34, no. 3, pp. 149–176, 2013.
- [13] S. Wan and R. Reilly. (2013, April) IEEE micromouse competition rules (region 1). <http://sites.ieee.org/r1/files/2013/03/2013-Region-1-Micromouse-Competition-Rules.pdf>. [Online]. Available: <http://sites.ieee.org/r1/files/2013/03/2013-Region-1-Micromouse-Competition-Rules.pdf>
- [14] S. Denei, F. Mastrogiorganni, and G. Cannata, "Towards the creation of tactile maps for robots and their use in robot contact motion control," *Robotics and Autonomous Systems*, vol. 63, Part 3, pp. 293 – 308, 2015, advances in Tactile Sensing and Touch-based Human Robot Interaction. [Online]. Available: <http://www.sciencedirect.com/science/article/pii/S0921889014001869>
- [15] R. Kümmerle, B. Steder, C. Dornhege, M. Ruhnke, G. Grisetti, C. Stachniss, and A. Kleiner, "On measuring the accuracy of slam algorithms," *Autonomous Robots*, vol. 27, no. 4, pp. 387–407, 2009. [Online]. Available: <http://dx.doi.org/10.1007/s10514-009-9155-6>
- [16] D. Ball and M. Milford. (2015, January) OpenratSLAM datasets. [Online]. Available: <https://wiki.qut.edu.au/display/cyphy/openRatSLAM+datasets>
- [17] D. Ball, S. Heath, G. Wyeth, and J. Wiles, "iRat: Intelligent rat animat technology," *Proceedings of the 2010 Australasian Conference on Robotics and Automation*, pp. 1–3, 2010.
- [18] B. Mitchinson and T. J. Prescott, "Whisker movements reveal spatial attention: Unified computational model of active sensing control in the rat," *PLoS Computational Biology*, vol. 9, no. 9, 2013.